

Swissgrid's strategic grid 2025 : an independent analysis

Laurent Pagnier¹ and Philippe Jacquod¹

¹School of Engineering, University of Applied Sciences of Western Switzerland HES-SO CH-1951 Sion, Switzerland

I. SUMMARY

In this report we perform an independent analysis of Swissgrid's strategic grid 2025. We study the reliability of the Swiss power system for different scenarios with high penetrations of renewable energy sources (RES) in Swiss and European energy mixes, corresponding to the year 2030 as currently anticipated. Our investigations show that the Swiss transmission network will be considerably less congested after the enhancement of the grid from its present configuration to the strategic grid 2025. We conclude that the latter seems to be appropriately calibrated.

II. LABELING

Lines in the transmission network are labelled by the first 5 letters of the corresponding substations followed by a number labeling its voltage : 1 for 380kV and 2 for 220kV lines. We use the term *connection* to describe more than one transmission line between two substations, e.g. the CHAMO2-RIDDE2 connection consists of 3 transmission lines, see Fig 1.

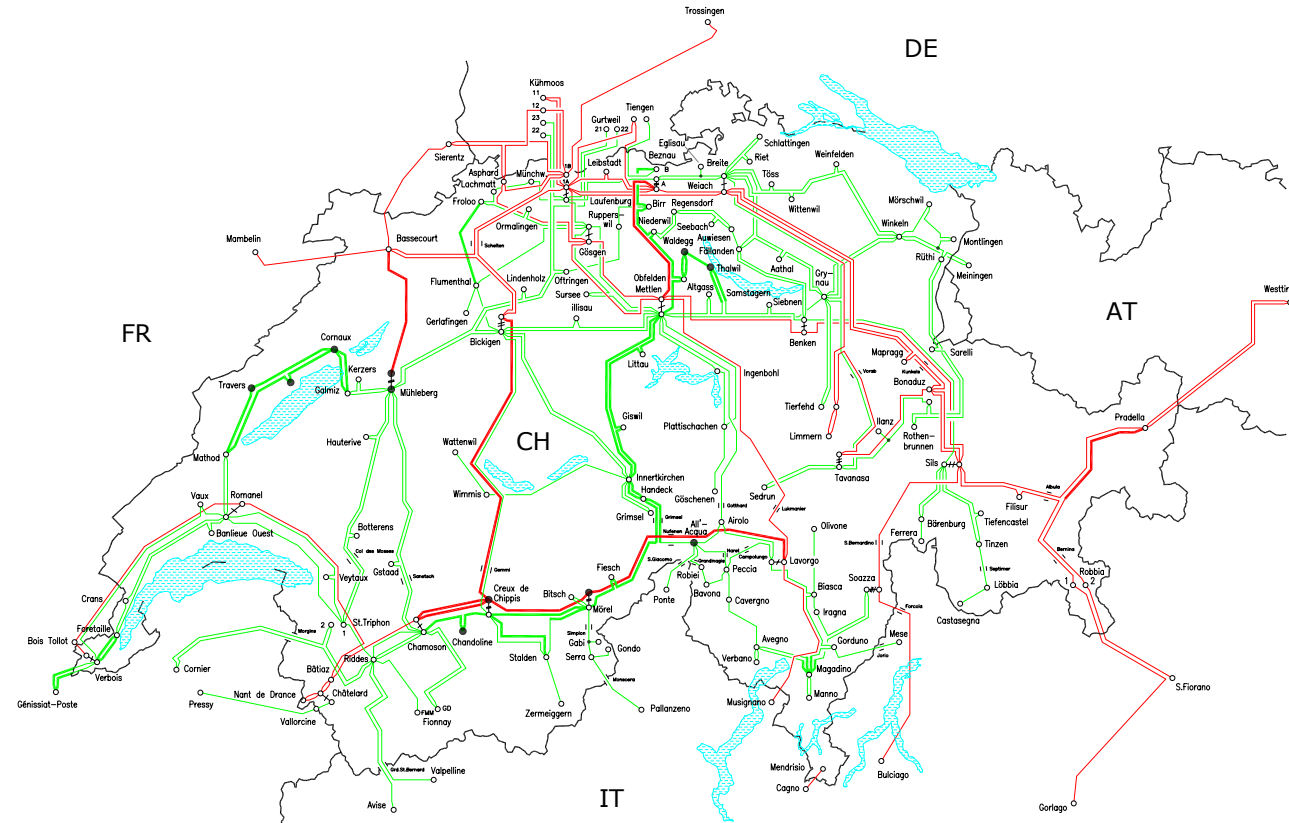


FIG. 1. The strategic grid 2025: 380kV and 220kV power lines are displayed in red and green respectively. Proposed new lines are in bold. (Source: Swissgrid)

The thermal power limit F_k^{\max} of a transmission line labelled k is obtained from its thermal maximal current, I_k^{\max} , as

$$F_k^{\max} = \sqrt{3}V_k I_k^{\max}, \quad (1)$$

where V_k is the nominal voltage of the line.

III. INTRODUCTION

Swissgrid is the owner and operator of the Swiss transmission network. Its missions are to guarantee the reliability of the grid and to allow electricity to be exchanged indiscriminately. To carry out these missions, Swissgrid must maintain, renew and if necessary extend the grid. In 2015, Swissgrid presented its strategic grid 2025 [1], which is the results of a two-step optimization. In the first step, the 2015 grid is enhanced progressively until the resulting grid is no longer congested. The upgrades considered are :

1. Where possible, the operating voltage is increased from 220kV to 380kV.
2. If transmission towers can carry an additional line, that line is added.
3. New lines are built.

In the second step, each upgrade element is removed sequentially and the influence of this removal on the reliability of the grid is assessed. A socioeconomic analysis is made in parallel, which weights how much each upgrade improves grid reliability against its cost. Based on the results, elements are kept or discarded. The result is the strategic grid 2025 which is displayed in Fig. 1. The main enhancements are stronger East-West and North-South connections, and a strengthening of the connection of western Switzerland to the 380kV network. In particular, new 380kV lines connect Valais to Ticino, and one of the existing lines between Valais and Bern is upgraded to 380kV.

IV. METHODOLOGY

In Refs. [2, 3], we developed a pan-European, aggregated grid model [see Fig. 2 (a)], where different types of production are dispatched following a merit order. We upgrade this model by disaggregating the Swiss power system, and embed the 220kV and 380kV transmission grids (the actual 2015 grid or the strategic grid 2025) inside the aggregated European grid [see Fig. 2 (b)]. We shortly describe our pan-European model and the modifications we made to incorporate the Swissgrid networks. More details can be found in Refs. [2, 3].

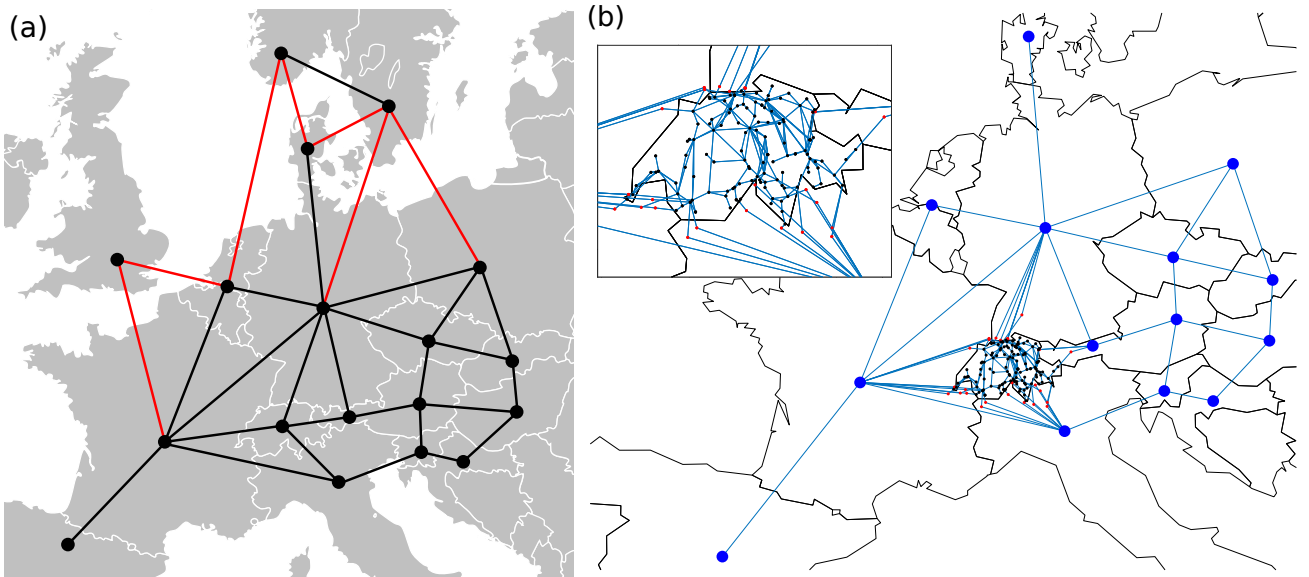


FIG. 2. (a) Aggregated model of the Central and Northern European grid. Each node represents an aggregated dispatch region. Lines represent interconnections: AC connections are in black and DC connections in red. (Figure taken from Ref. [2].) (b) The Swiss high voltage transmission network is embedded into our aggregated model of the pan-European power grid.

Equivalent aggregated models have a relatively long history [4–6]. They are standardly used for systemic investigations such as ours, where precise details of power flows are not crucial (as opposed to, say, grid stability investigations) and exact, geographically resolved production and consumption data are hard to obtain. In our case, we are not interested in detailed flows outside Switzerland but still want to account semi-realistically for power flows surrounding Switzerland. Simultaneously, we do not want to rely too much on arbitrary choices for the geographical distribution of loads within European countries. We therefore choose to use an aggregated European model.

A. Aggregated pan-European electric grid

Fig. 2 (a) shows our aggregated European grid, with each node representing an independent dispatch region (Portuguese consumption and production are included in the Spanish node). Aggregated lines have admittance (either for the 2015 grid or the strategic grid 2025) obtained via a standard reduction method [7] and thermal limits are given by the sum of the physical lines they represent. The power flows are computed in the DC lossless approximation [8].

B. Productions and Consumptions

Consumptions and productions are aggregated within each dispatch region and attributed to the corresponding node. Power productions are subdivided into two sets. They are,

- Non-flexible productions, mostly consisting of run-of-the-river (RoR), solar photovoltaics (PV) and wind turbine productions, as well as "miscellaneous productions". RoR is in principle flexible to some extent, but here we choose to neglect curtailment and consider that, as for PV and wind turbines, RoR production is determined by weather/seasonal conditions only.
- Flexible productions: We classify them into 6 types, which are (i) dam hydroelectricity, (ii) pumped-storage hydroelectricity (which can be positive as well as negative, but always counted as a production), (iii) gas and oil, (iv) nuclear, (v) hard coal and (vi) lignite productions. Each of these productions is characterized by a ramp rate (up/down) which is discussed below.

For each region labelled i and at each time t , we define the residual loads $R_i(t)$ as the difference between the consumption and the non-flexible productions,

$$R_i(t) = L_i(t) - P_i^{\text{inflex}}(t), \quad (2)$$

where $L_i(t)$ and $P_i^{\text{inflex}}(t)$ give the load and the sum of the non-flexible productions respectively. Our task is to dispatch flexible productions so that their production is equal to the total residual load at all times - this is equivalent to balancing consumption with production.

C. Economic dispatch

A large number of different optimized power flows exist [9–13]. Our dispatch algorithm follows a merit order. The latter is based, first, on marginal costs, a^k , specific to each production type, k . Second, we introduce effective parameters in the form of repulsion costs, b^k , which progressively increase the total production cost as the production increases and reaches its maximal possible value. Such repulsion costs do not directly correspond to any real economic cost, however we found that they are necessary to smoothen production curves and reproduce historical time series faithfully. With these two parameters for each of the six different flexible productions, our model has a total of 12 parameters that need to be calibrated. Refs. [2, 3] showed that historical production profiles for all flexible productions in different European countries are well reproduced once these parameters are properly calibrated. To illustrate the validity of our model we present a comparison of historical and calculated hydroelectric production profiles in Norway and Switzerland in Fig. 3.

The production cost in the i^{th} region at each time step $\Delta t = 1\text{h}$ is given by a sum over the marginal and repulsion costs for all production types as

$$W_i(t) = \sum_k \left[a^k P_i^k(t) + b^k \frac{P_i^k(t)^2}{P_{\max i}^k} \right] \Delta t, \quad (3)$$

where $P_i^k(t)$ is the power generated by a given production type labelled k , in a geographical region labelled i , at time t , and $P_{\max i}^k$ is the corresponding installed capacity. Our algorithm is based on an optimal power flow which determines the production profiles $\{P_i^k(t)\}$ minimizing the total, annual generation cost

$$W(\{P_i^k(t)\}) = \sum_{i,t} W_i(t), \quad (4)$$

under the following technical constraints:

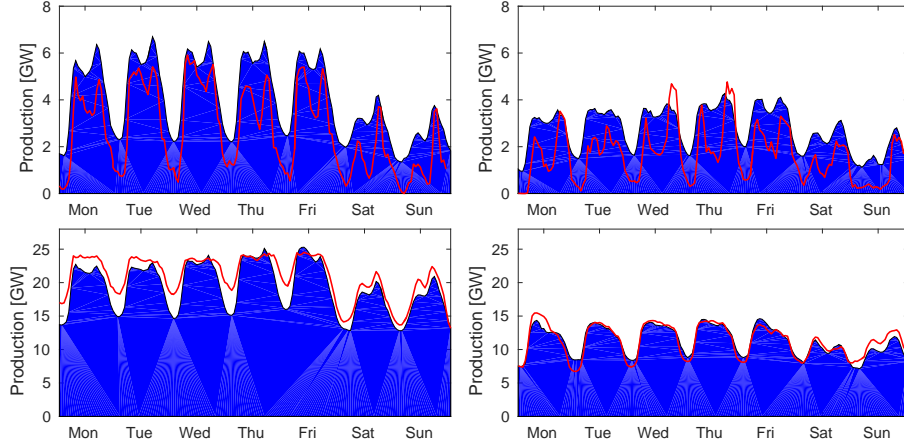


FIG. 3. Dam production of Switzerland (top) and Norway (bottom) for a week in winter (left) and summer (right) in 2015. Dispatched productions are displayed in blue and actual 2015 production profiles are in red.

- a. *Power limits* $P_i^k(t) \leq P_{\max i}^k, \forall t$; the power generated never exceeds its maximal installed capacity.
- b. *Ramp rates* $|\partial P_i^k(t)/\partial t| \leq \Gamma_i^k, \forall t$; each production type has a maximal ramp rate Γ_i^k at which the production increases or decreases. These ramp rates are similar, but not exactly equal, to the real, technical rates. We adapted them slightly when calibrating our model, to reproduce historical production time series better.
- c. *Internodal power flows* $|F_k(t)| \leq F_k^{\max}$; they should never exceed the thermal limit F_k^{\max} between regions.
- d. *Dam storage* Dam hydroelectric plants are constrained by the finiteness of their reservoir and the annual water intake into the latter.

The pumped-storage (PS) plants have no marginal cost. The price of electricity gives them the signal whether they must pump or generate and its variations allows them to generate profits. We showed that the residual load, defined in Eq. (2), is strongly correlated to the day-ahead electricity price [14]. Consequently, one can define an effective electricity price $p_{\text{eff } i}(t)$ based on the residual load. In the i th region, the revenues $G_{\text{PS } i}$ generated by the PS plants in this region depend on their pump/turbine powers $P_{\text{pi}}(t)$ and $P_{\text{ti}}(t)$ and the filling $S_{\text{PS } i}(t)$ of their reservoirs as

$$G_{\text{PS } i} = \sum_k p_{\text{eff } i}(t_k) [P_{\text{ti}}(t_k) - P_{\text{pi}}(t_k)] \Delta t \quad (5)$$

$$\text{s.t. } 0 \leq S_{\text{PS } i}(t_k) \leq S_{\text{PS } i}^{\max}, \forall k. \quad (6)$$

At each time step $\Delta t = 1\text{h}$, the reservoir filling evolves as

$$S_{\text{PS } i}(t + \Delta t) = S_{\text{PS } i}(t) + [\eta P_{\text{pi}}(t) - \eta^{-1} P_{\text{ti}}(t)] \Delta t, \quad (7)$$

with a typical pump/turbine efficiency of $\eta = 0.9$ (each way). We define a cost function for PS operations as

$$W_{\text{PS}} = - \sum_i G_{\text{PS } i}. \quad (8)$$

We add this term to the cost function defined in Eq. (4), after which our economic dispatch minimizes the total production cost while maximizing the revenues of the PS plants.

D. Disaggregation of Switzerland

Effective admittances are determined for lines between Swiss buses and the aggregated European buses. They are chosen so that, with historical power injections in Switzerland and Europe, numerically obtained power flows on these lines are close to the corresponding historical power flows. Fig. 4 illustrates how well this calibration process works.

For lines inside Switzerland, we use their true admittances. Our economic dispatch determines the total production for each production type. The power flow computations require geographical resolution, i.e. power injections at each bus, which we obtain as follows. For a given production type, labelled k , the rated power connected to the grid bus

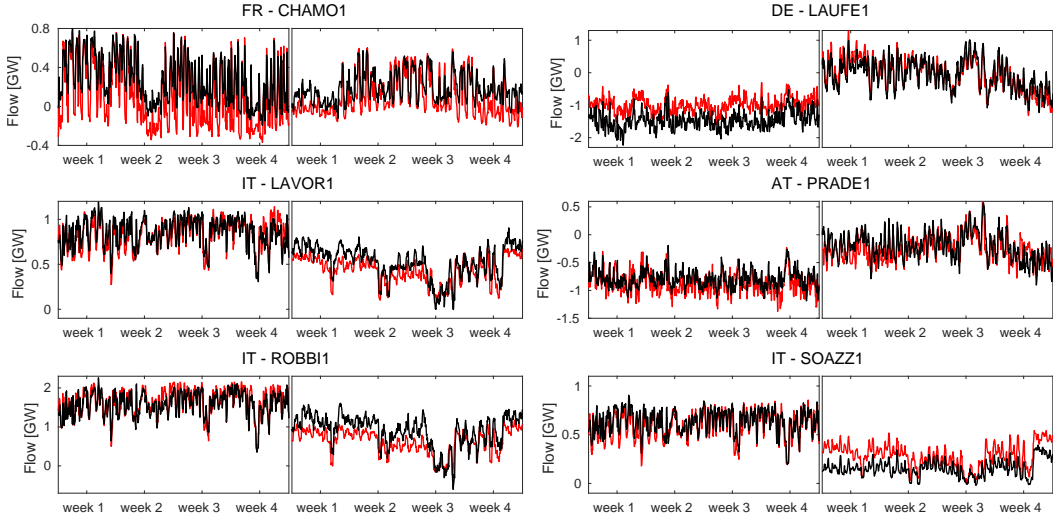


FIG. 4. Calculated (red) vs. historical (black) power flows on six different interconnections to Switzerland for four winter (left panels) and four summer weeks (right panels) in 2015.

number i is given by $P_{\text{rated } i}^k$. The distribution factor π_i^k is defined as

$$\pi_i^k = \frac{P_{\text{rated } i}^k}{P_{\text{rated CH}}^k}, \quad (9)$$

where $P_{\text{rated CH}}^k$ is the Swiss nameplate capacity of this type of production. Then, the power injection $\Pi_i(t)$ in the i th bus is given by

$$\Pi_i(t) = \sum_k \pi_i^k P_{\text{CH}}^k(t) - R_i(t). \quad (10)$$

Here, $R_i(t)$ is the residual load at bus number i , defined as the difference between the true 2015 load and the numerically modeled RES productions. More information on the model, its calibration and validation can be found in Ref. [2].

E. Comparison with Swissgrid's methodology

To assess the strategic grid 2025 against the current one, Swissgrid did 2-step simulations. The first step is a market simulation. The productions are dispatched at (aggregated) national scale. Once the national productions are determined, they are distributed to the buses of a (nonaggregated) pan-European grid. This distribution process is to some extent arbitrary (though checks have been made that show a relatively low impact on power flows on the swiss very high voltage power grid). We circumvent this difficulty and introduce an aggregated model.

We are particularly interested in assessing future uses of pumped-storage facilities, and note that our model has hourly resolution of PS dispatch based on modelized spot market prices [see the discussion in Section IV C and in particular Eq. (7)]. This seems to go beyond the methodology used in Swissgrid's report on the 2025 strategic grid [15].

V. SCENARIOS

We consider scenarios for the year 2030, when the energy transition will be well underway. For Switzerland, this means in particular that all but one nuclear power plant (Leibstadt) are decommissioned. The corresponding missing productions are substituted either by new RES or imports. We focus on scenarios with high penetrations of renewable energy sources (RES). We expect that if the grid is resilient to these scenarios, there won't be problems for more business as usual (slow progress) scenarios.

A. Europe

We base our simulation on 2015 data from the association of European transmission grid operators (ENTSO-E) [16]. We complement these data with informations provided by different European transmission system operators. Population growth drives consumption up, however higher energy efficiency decreases it. We assume these factors to compensate each other so that the loads of European countries remain relatively constant. Accordingly, we use the load of 2015 without modification. ENTSO-E publishes data on historical production and load profiles and installed capacities in the different countries [16] and forecasts for future production capacities [17, 18]. We use these forecasts to set up the production capacities in each country in Fig. 2 (a).

B. Switzerland

Our study is based on actual data we obtained from Swissgrid with the topology of the Swiss transmission network and the production and consumption profiles at each bus for each hour of 2015. The loads on the Swiss buses are used without any modification. The capacity of dam hydroelectricity remains unchanged. All nuclear power plants, except Leibstadt, are decommissioned. The Nant-de-Drance and Linth-Limmern PS plants are connected to the grid (meaning in particular that we artificially add a substation at La Batiaz to connect Nant-de-Drance to the 380kV grid in the 2015 grid). Our Swiss RES production profiles rely on the wind speed and solar irradiance profiles at several locations in Switzerland, taken from the IDAWEB database [19].

Most of the projects of new wind turbines in Switzerland are located in the Jura Mountains, therefore we consider new wind turbines only there. The production of a wind turbine is obtained from the wind speed with the following power curve

$$P^{\text{tur}}[v(t)] = \begin{cases} P_{\text{rated}}, & \text{if } v_{\text{rated}} \leq v(t) < v_{\max}, \\ P_{\text{rated}}/v_{\text{rated}}[v^3(t) - v_{\min}^3], & \text{if } v_{\min} \leq v(t) < v_{\text{rated}}, \\ 0, & \text{otherwise.} \end{cases} \quad (11)$$

where P_{rated} and v_{rated} are the rated power of the turbine and the corresponding rated speed, v_{\min} is the minimal wind speed at which the turbine produces, v_{\max} is the cut-out speed above which the turbine is stopped. In the following we use $P_{\text{rated}} = 1[\text{p.u.}]$, $v_{\min} = 3[\text{m/s}]$, $v_{\text{rated}} = 14[\text{m/s}]$ and $v_{\max} = 25[\text{m/s}]$. To obtain the Swiss wind production, we compute the production of 100 wind turbines. We need to take into account the fact that two wind turbines are always subjected to different winds, whereas there are only a few weather station in the Jura Mountains that give us wind time series. To each wind turbine we therefore attribute a wind profile that is defined as the sum

$$v_i(t) = v_i^{\text{ws}}(t) + W(i, t), \quad (12)$$

of the true wind speed $v_i^{\text{ws}}(t)$ at some weather station and a white noise term $W(i, t) \in [-W_0, W_0]$, with W_0 chosen so that the noise term does not dominate. The total wind production is given by

$$P^{\text{WT}}(t) = \xi^{\text{WT}} \sum_{i=1}^{100} P^{\text{tur}}[v_i(t)], \quad (13)$$

where ξ^{WT} normalizes the total wind production profile in order to obtain the desired annual production. As no information on the topology of the distribution network is available, it is not possible to anticipate exactly where the production of a wind turbine is injected in the transmission network. We assume a distribution as summarized in Table I.

bus name	[%]
BASSE1	33
MATHO2	33
KERZE2	11
GALMI2	11
HAUTE2	6
PIETE2	6

TABLE I. Percentage of injection of wind turbine production per bus.

Solar photovoltaics will be dominantly installed on rooftops in Switzerland. Therefore we distribute the PV production demographically. One can argue that the urban regions with higher population density (i.e. where people live in larger residential buildings rather than in individual dwellings), have lower roof surface per capita ratios. However, there are usually commercial or industrial parks in the vicinity of urban regions offering important roof surfaces. For the sake of simplicity, we assume that these two aspects balance each other. The PV production at each bus is the sum of the contributions of all municipalities connected to it via the low- and medium-voltage grids. We assume that each municipality is served by its nearest bus. The contribution of the i th municipality depends on its population and its solar irradiance $\text{SI}_i(t)$ which is obtained as the weighted average of the solar irradiances at the nearest weather stations

$$\text{SI}_i(t) = \frac{1}{N} \sum_{d_{ij} < d_{\max}} \frac{1}{d_{ij}} \text{SI}_j^{\text{ws}}(t), \quad (14)$$

where $\text{SI}_j^{\text{ws}}(t)$ is the solar irradiance at the j th weather station, d_{ij} is the distance between the i th municipality and the j th weather station, $d_{\max} = 40\text{km}$ is an arbitrarily chosen threshold distance and $N = \sum_{d_{ij} < d_{\max}} d_{ij}^{-1}$. This procedure prevents local perturbations from affecting too strongly PV production and its injection at buses. The contribution $\text{PV}_i(t)$ of the i th municipality depends on its population pop_i and is given by

$$\text{PV}_i(t) = \frac{\text{pop}_i}{\text{pop}_{\text{tot}}} \text{SI}_i(t), \quad (15)$$

where pop_{tot} is the Swiss population. Each municipality contributes to the PV production of its closest bus. The PV production at the k th bus is given by

$$P_k^{\text{PV}}(t) = \xi^{\text{PV}} \sum_{i \in I_k} \text{PV}_i(t), \quad (16)$$

where I_k is the set of indices of the municipality related to the k th bus and ξ^{PV} uniformly scales to meet the planned annual production.

We define two scenarios of development of RES in Switzerland. In both cases, we assume that the energy transition in Switzerland will mainly rely on solar power to replace nuclear production. To do so, our first scenario relies on solar power exclusively. In the second scenario, we reduce the PV production by 4TWh which are produced by about 600 large wind turbines instead. In both scenarios the annual RES production is 17TWh, corresponding to the average annual nuclear production minus the Leibstadt production. The characteristics of our two scenarios are summarized in Table II.

	PV [TWh]	WT [TWh]
100% PV scenario	17	0
RES mix scenario	13	4

TABLE II. Swiss PV and wind turbine (WT) annual productions in the 2 scenarios considered in this report.

VI. RESULTS

A. Normal N operation

We perform numerical simulations with and without thermal power limits on the Swiss transmission grid. Just as is the case in real life, more constraints means that a redispatch is sometimes necessary. By comparing simulations with and without constraints, we can determine if the producers, in particular hydroelectric producers, are limited in their operations by grid constraints and the associated necessary redispatch.

Fig. 5 shows histograms of congestions for unconstrained power flows on the Swiss transmission network for the 2015 grid and for the strategic grid 2025. Panel (a) gives the number of hours per year when the flow on some line exceeds a given value (normalized with the thermal limit of that line) while panel (b) shows the number of hours when a given number of lines exceeds their thermal limit. With the strategic grid 2025, there is no congestion almost 90% of the time (compared to less than 70% for the 2015 grid) and there is never more than one overloaded line. With the 2015 grid there are more than 3 simultaneously overloaded lines 2% of the time.

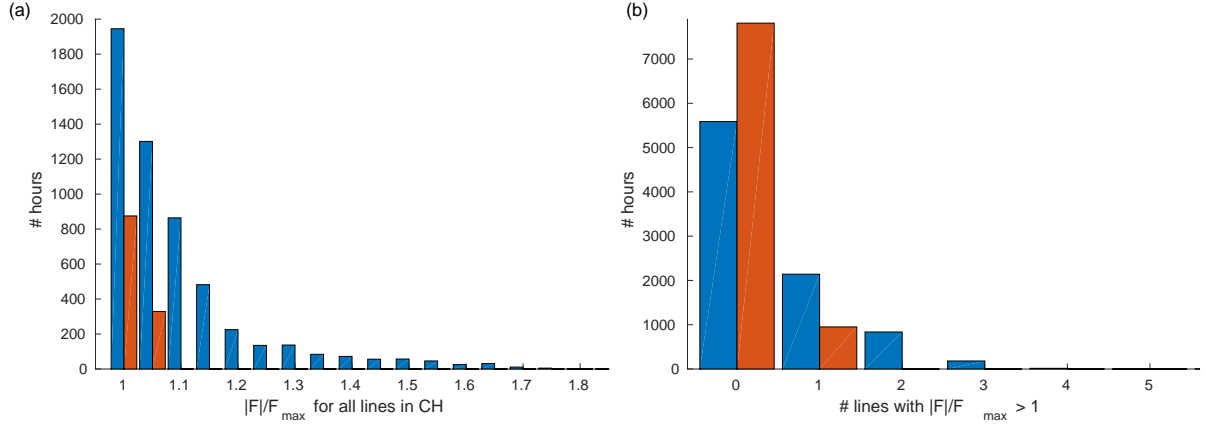


FIG. 5. Hours of congestion in the 2015 grid (blue) and strategic grid 2025 (red) for unconstrained swiss flows simulations as a function of the line load [Panel (a)] and the number of overloaded lines [Panel (b)].

The strong and frequent overloads in the 2015 configuration cannot be tolerated. They would require a heavy recourse to redispatching, and in worst cases, could require load shedding or even lead to blackouts. Fig. 5 demonstrates that the strategic grid 2025 strongly suppresses the congestions, that overloads occur less often and that their magnitude is strongly reduced. The significant problems that plague the 2015 grid are clearly fixed with the strategic grid 2025, where only few, moderate overloads occur. As a sideremark, we conclude that unconstrained flow simulations with the 2015 grid are unrealistic – constraints leading to different dispatches must be considered when doing numerical simulations with that grid.

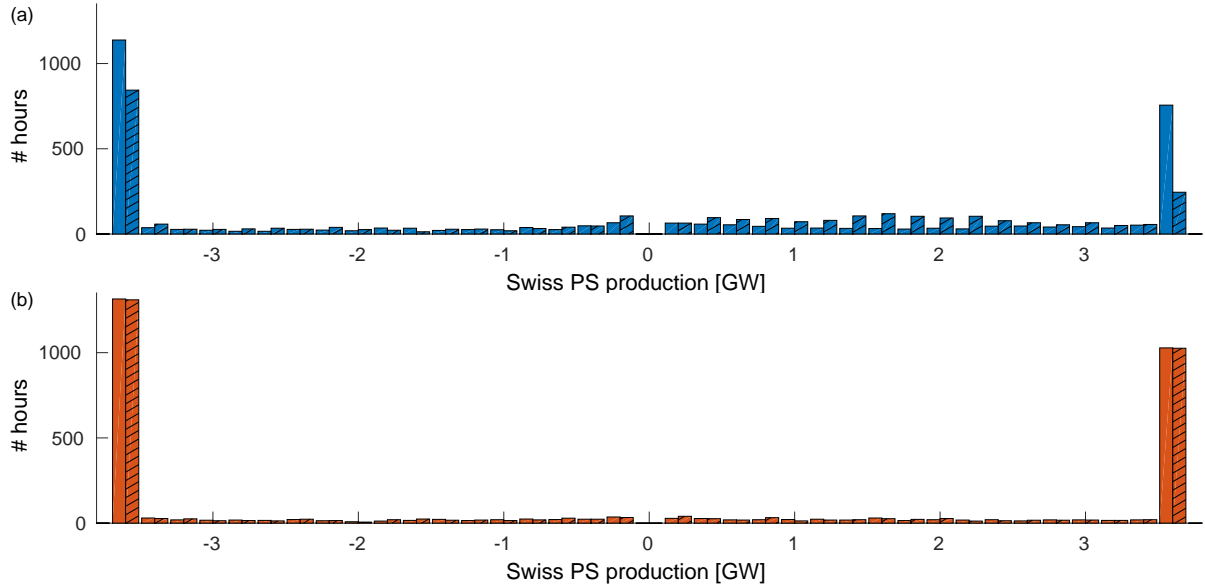


FIG. 6. Histograms of the production of Swiss PS plants with (hatched) and without (plain) constraints on the power in the 2015 grid [panel (a)] and in the strategic grid 2025 [panel (b)]. Negative production means pump consumption and in both panels, the idle state spike has been removed. The annual pump consumption is higher than the annual production due to a finite efficiency of $\eta = 0.9$ each way.

We next investigate PS production in the 2015 and 2025 grids. Fig. 6 (a) shows the Swiss PS production with the 2015 grid. When the Swiss flows are constrained – the only realistic calculation, as just discussed – the usage of the PS facilities is reduced by 18% and PS plants can only rarely produce at full power. The situation significantly improves with the 2025 grid, as can be seen in Fig. 6 (b), where flow constraints affect PS production only weakly. Calculated with the procedure defined in Refs. [2, 3], revenues of PS plants are down by 17% with the 2015 grid compared to

their revenue with the strategic grid 2025. Clearly, the strategic grid 2025 is beneficial for PS operators, who will be able to operate their facilities almost without grid constraints.

To conclude this section on normal, N operation, we finally zoom in on a specific aspect of hydroelectric production in Valais. Fig. 7 shows the power flowing through the 220/380 kV transformer at the Chamoson substation when the Swiss flows are unconstrained. In the 2015 grid, it is overloaded more than 18% of the time, while there is no overload with the strategic grid 2025. Accordingly, dispatch would put significant constraints on hydroelectricity production with the 2015 grid, but almost none with the strategic grid 2025.

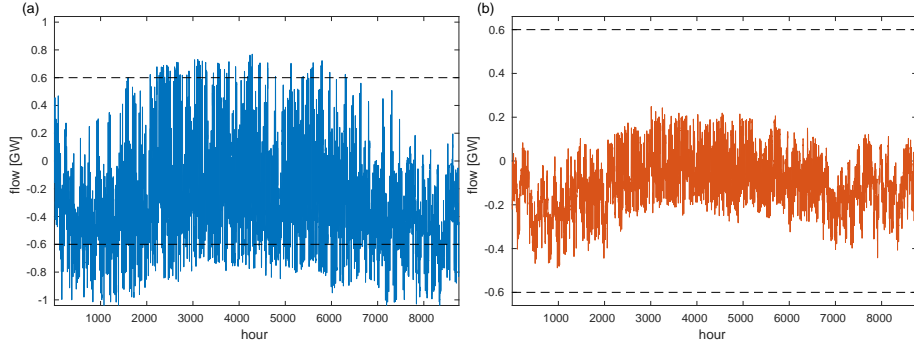


FIG. 7. Power flow through the transformer at Chamoson substation for unconstrained flow simulation in the 2015 grid (left) and with the strategic grid 2025 (right). Dashed lines represent the power limit of 0.6 GW. Positive flows go to the 380kV level, negative ones to the 220 kV level.

B. Power flow with $N - 1$ contingencies

We next perform $N - 1$ contingency calculations. Each line of the Swiss network is cut sequentially, and a power flow calculation with the resulting network is performed. We define the worst case $N - 1$ flow $F_k^{N-1}(t)$ for the k th line at time t as

$$F_k^{N-1}(t) = \max_{i=\{1, \dots, N_{\text{line}}\}} (|F_{i,k}(t)|) \forall t, \quad (17)$$

where $F_{i,k}(t)$ is the power flow on the k th line after line i is cut.

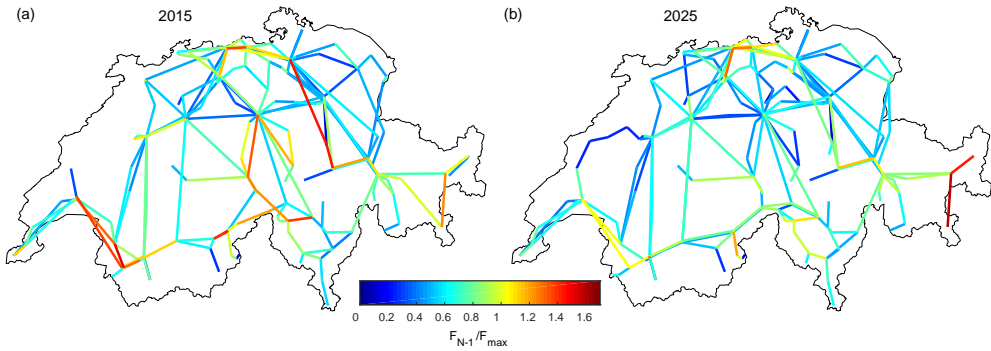


FIG. 8. (a) Annual N-1 maximal flows in the 2015 grid. (b) Annual N-1 maximal flows in the strategic grid 2025. All flows are obtained with the 100% PV scenario.

Fig. 8 (a) shows the annual maximal $N - 1$ power flows in the 2015 grid. We observe that the grid is strongly congested on several lines. This is particularly the case in sections of the grid connected to large hydro power plants. Fig. 8 (b) shows that the strategic grid 2025 strongly reduces these congestions. Still, the PRADE1-ROBBI1 connection gets overloaded sometime by the North-South transit.

Fig. 9 further shows the worst case $N - 1$ power flows for 10 of the most heavily loaded transmission lines. With the strategic grid 2025, flows remain below their thermal limits almost always. Note that these results are essentially

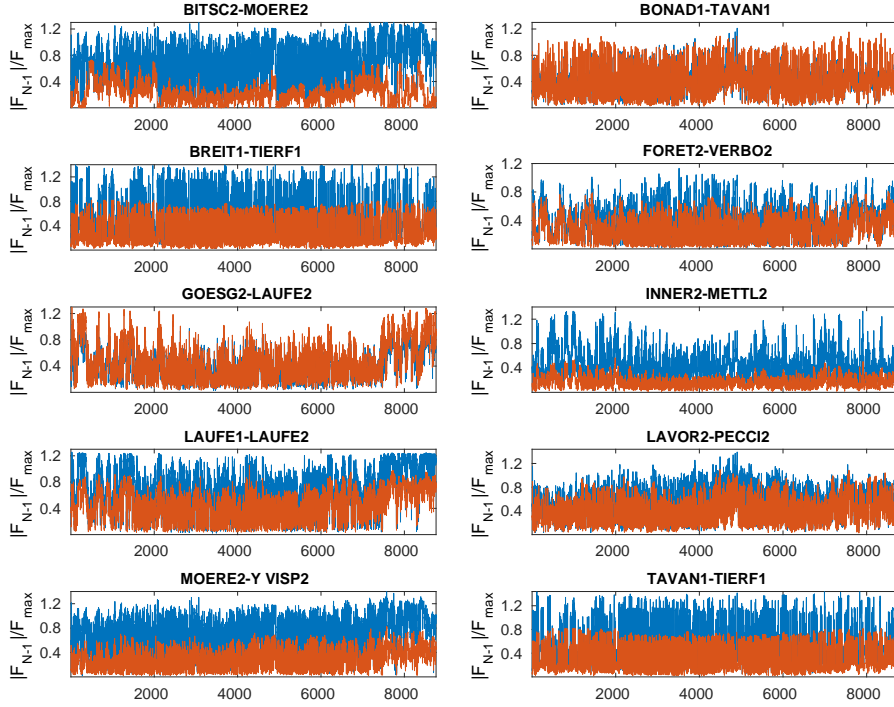


FIG. 9. Worst case N-1 power flows in the 2015 grid (blue) and in the strategic grid 2025 (red) for 10 of the most heavily loaded lines.

the same, whether one considers our 100% PV scenario or the RES mix (PV and 4TWh wind turbine production) scenario.

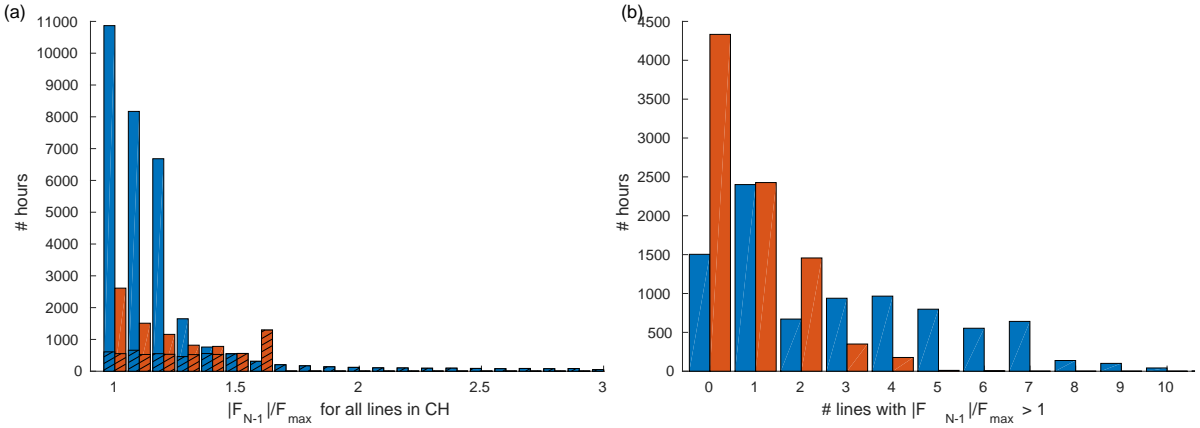


FIG. 10. (a) Hours of congestion in the 2015 grid (blue) and strategic grid 2025 (red) for worst case N-1 power flows, as a function of the maximal line overload [Panel (a)] and the number of simultaneously overloaded lines [Panel(b)]. The hatched areas in the left panel represent the contribution of the single most overloaded line for both grids (the BATIA1-CHAMO1 line for the 2015 grid and the ROBBI1-LAPUN1 connection for the strategic grid 2025).

Fig. 10 shows histograms for the duration of the worst case $N - 1$ congestions for the 2015 and the strategic grid 2025 as a function of the load on lines [Panel (a)] or the number of simultaneously overloaded lines [Panel (b)]. Panel (a) shows that the 2015 grid is very significantly more often overloaded, especially for relatively weak overloads, $F_{N-1}/F_{\max} < 1.3$, as well as for strong overloads, $F_{N-1}/F_{\max} > 1.6$. For intermediate overloads, both grids perform similarly. More detailed analysis shows that a significant fraction of the overloads occurs on the transformer at the Chamoson substation for the 2015 grid (when the BATIA1-CHAMO1 line exiting Chamoson trips out) and on the

ROBBI1-LAPUN1 connection (when one of its two lines trips out) for the strategic grid 2025 – the contribution from these overloads is indicated by hatches in Fig. 10(a). In particular, the overloads on the ROBBI1-LAPUN1 connection are solely responsible for the peak at $F_{N-1}/F_{\max} = 1.6$ for the strategic grid 2025. Finally, Fig. 10 (b) shows that $N - 1$ overload events are much rarer with the strategic grid 2025, where they occur 50% of the time, compared to more than 80% of the time with the 2015 grid. The 2015 grid has 3 or more overloaded lines more than 40% of the time, compared to only 6% for the strategic grid 2025. Additionally, the strategic grid 2025 has never more than 4 simultaneously overloaded lines in $N - 1$.

We next perform some stretch test and look into somehow exceptional production periods over Europe. The $N - 1$ contingency analysis shown from here on focuses on the strategic grid 2025. Fig. 11 (a) shows simulated dispatched

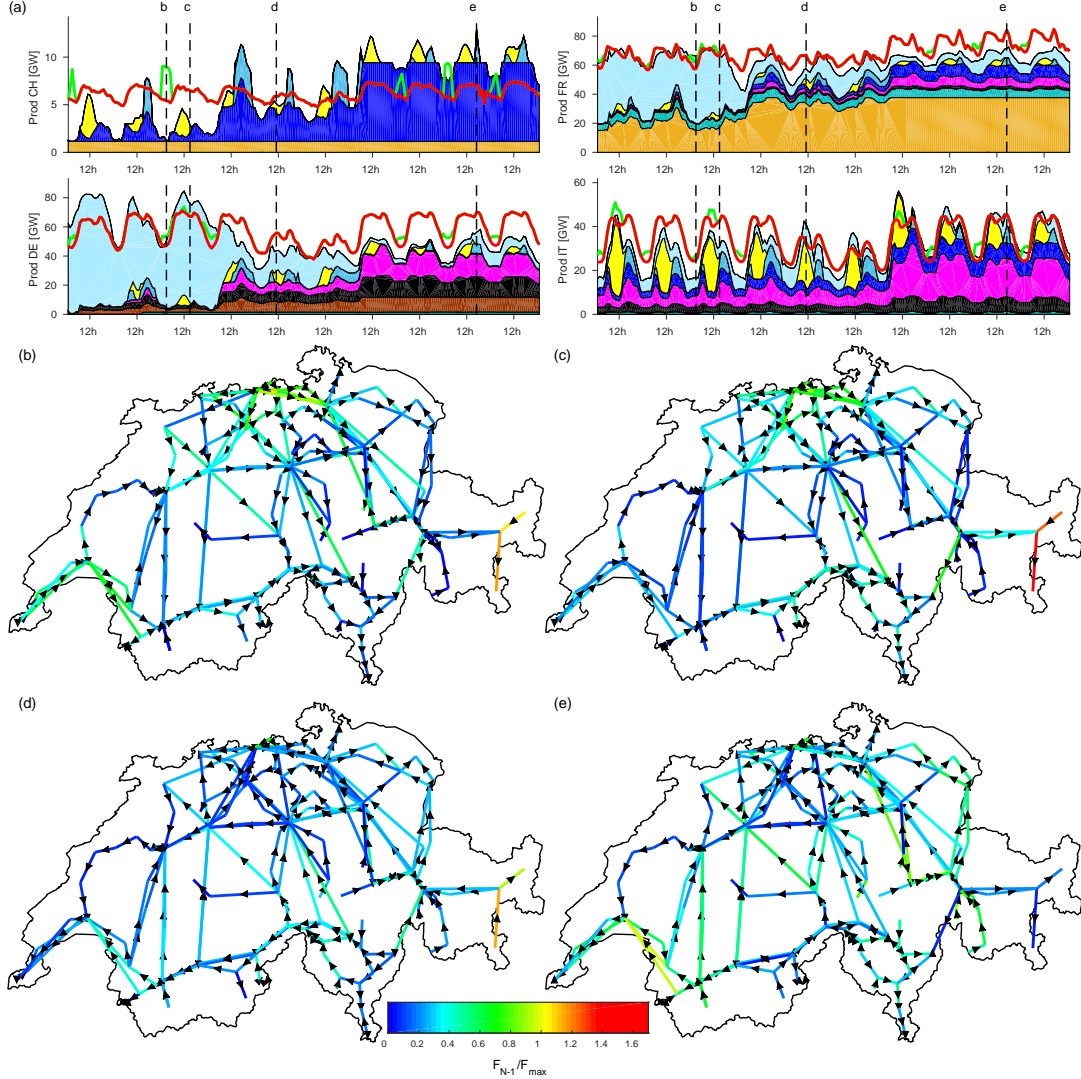


FIG. 11. (a) Production and consumption profiles in Switzerland, France, Germany and Italy for 10 days in winter. Production types are color-coded as follows : lignite (brown), hard coal (black), nuclear (orange), gas (magenta), run-of-the-river (cyan), dam (deep blue), solar power (yellow), wind power (light blue) and PS generation (turquoise). The red and green lines represent the loads of the different countries and the additional load due to the PS pumps respectively. Panels (b)-(e) show the worst $N - 1$ power flows for the strategic grid 2025, for times indicated by vertical dashed lines in panel (a).

productions of Switzerland, France, Germany and Italy for ten consecutive days in winter. During the first three days, the RES production in Europe is high, in particular from wind power. Wind turbine generation in Germany is actually sufficient to cover alone the whole German load during the first day shown. During that time, hydroelectricity production in Switzerland is low and almost zero during offpeak periods. RES production in Europe decreases over the next three days. Dispatchable productions start to produce more to compensate this decrease. In the last 4 days shown, RES productions in Europe are low. Hydroelectricity in Switzerland produces near or at its maximal power

most of the time. Fig. 11 (b)-(e) present snapshots of the maximal N-1 power flows corresponding to times indicated by dashed lines in panel (a). In the situation described in panels (b) and (c), the Swiss production is very low, with essentially only Leibstadt producing. The Swiss load is 8.5 GW higher than the national production, while at the same time, Italy is strongly importing too. Even under these exceptional conditions, we see that the strategic grid 2025 behaves well and very few, very localized congestions occur - mostly the ROBBI1-LAPUN1 connection.

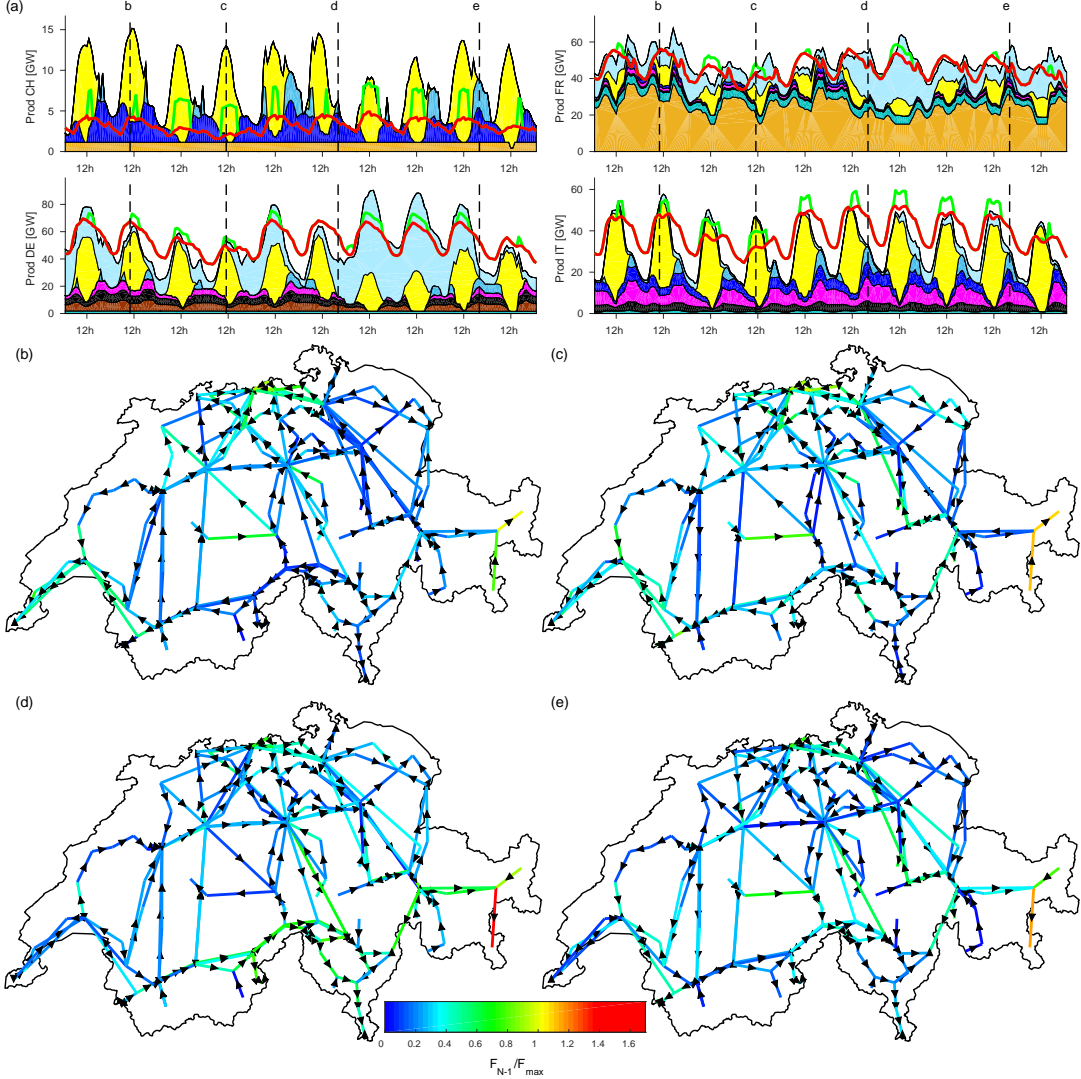


FIG. 12. (a) Production and consumption profiles in Switzerland, France, Germany and Italy for 10 days in summer. Production types are color-coded: lignite (brown), hard coal (black), nuclear (orange), gas (magenta), run-of-the-river (cyan), dam (deep blue), solar power (yellow), wind power (light blue) and PS generation (turquoise). The red and green lines represent the loads of the different countries and the additional load due to the PS pumps respectively. Panels (b)-(e) show the worst $N - 1$ power flows for the strategic grid 2025, for the times indicated by vertical dashed lines in panel (a).

Fig. 12 (a) shows the production of Switzerland, France, Germany and Italy for ten consecutive days, this time in summer. Italy and Switzerland which have high penetration of PV in their mixes, have large production around midday. Italy uses its PS pumps every day at noon and its PS turbines in the evening. Comparing Figs. 11 (e) and 12 (b), one observes that the Swiss peak production in summer exceeds by far that of winter, with production peaks at 15GW. Nevertheless the grid is less congested in summer, which we attribute to the geographically homogeneous spreading of the PV production in the grid.

Besides the rare, rather exceptional production times just considered, we investigated even more exceptional situations such as the one which occurred in winter 2016-2017, when 18 of the 58 French nuclear reactors were temporarily off the grid. Even coupled with different extreme scenarios for RES productions in France, Germany and Italy tailored to increase power transits in Europe, such exceptional situations were relatively easily sustained by the strategic grid

2025, with only few $N - 1$ congestions. We do not show these results here but would be happy to produce and discuss them upon request.

C. Chamoson-Chippis power line

Valais is the canton with the largest share of the Swiss hydroelectricity production. There are 13 power plants connected to the 220kV network which correspond to more than 2.4GW. Currently the only power plant connected to the 380kV network is Bieudron (~ 1.3 GW). The Nant-de-Drance power plant will be commissioned in 2020, which will increase the power capacity connected to the 380kV grid to about 2.2GW. There are 12 transmission lines at 220kV exiting Valais, corresponding to a total interconnection of roughly 6GW. This is much more than the total capacity injecting at this voltage level. On the other hand, there is in the 2015 grid only a single transmission line exiting Valais at 380kV. If that line fails, power has to be transformed to 220kV at the Chamoson substation. The worst case $N - 1$ power flows through that transformer are shown in Fig. 13. There are much fewer, much less severe overloads of that transformer with the strategic grid 2025, thanks to the new 380kV power lines connecting Valais to Ticino and Bern in the strategic grid 2025.

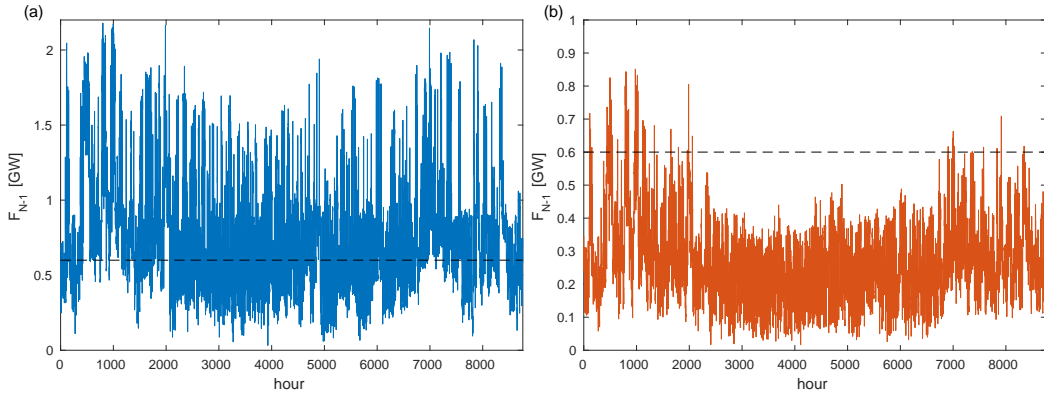


FIG. 13. Profile of the worst case $N - 1$ power flow through the transformer at Chamoson substation for the 2015 grid (left) and the strategic grid 2025 (right). Note that the worst case flow is by definition positive [see Eq. (17)].

Fig. 14 shows the profile and histogram of the worst case $N - 1$ power flow on the existing CHAMO2-CHIPP2 connection. This connection is heavily loaded, with the thermal power limit being exceeded about 100 hours a year. Fig. 15 shows the worst case $N - 1$ flow on the CHAMO1-CHIPP1 connection of the strategic grid 2025, when one

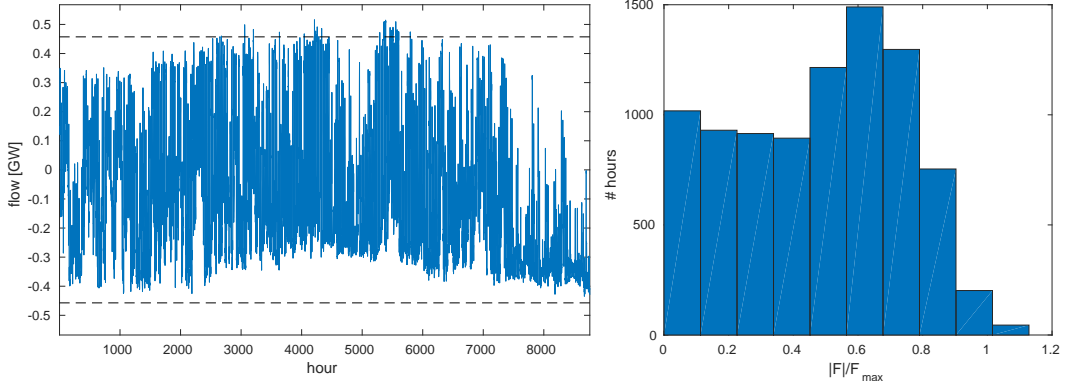


FIG. 14. Profile (left) and histogram (right) of the worst case $N - 1$ power flow on the CHAMO2-CHIPP2 connection, when one of its two lines trips out with the 2015 grid. Dashed lines represent the thermal power limit.

of its two lines trips out. There is a 20% margin to the thermal power limit all year long and even more most of the time. That margin means that, even with the uncertainties in our model and the assumptions on which it is based

there will not be many grid constraints on hydroelectricity production thanks to this new connection. The strategic grid 2025 seems to guarantee that hydroelectric production will not be constrained by the grid.

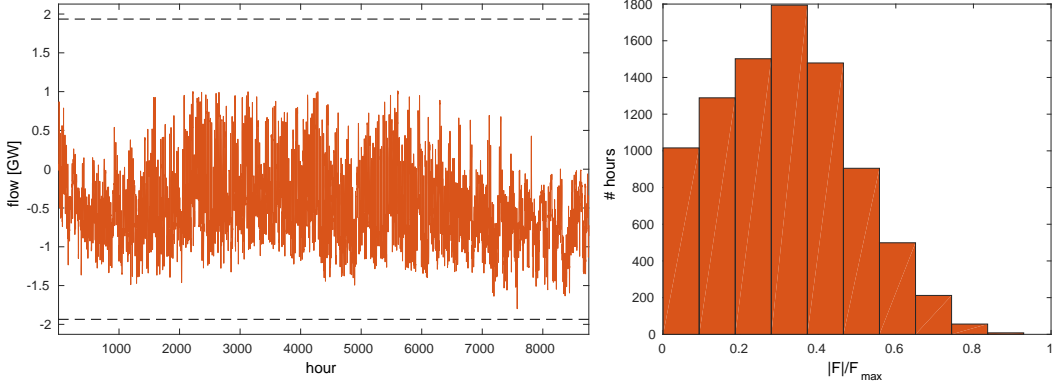


FIG. 15. Profile (left) and histogram (right) of the worst case $N - 1$ power flow on the CHAMO1-CHIPP1 connection, when one of the two lines constituting this connection is tripped out with the strategic grid 2025. Dashed lines represent the thermal power limit.

VII. CONCLUSION

In this report we constructed an aggregated model of the pan-European transmission grid in which we embedded the Swiss network. We created RES production profiles for every Swiss bus, based on its location and data from weather stations. We used our model to compare the 2015 grid and strategic grid 2025 of Switzerland.

The 2015 grid would be strongly congested in a future with high RES penetration. Hydroelectricity plants would be forced to reduce their production to guarantee the reliability of the grid. This is no longer the case with the strategic grid 2025. We conclude that the upgrade of the grid makes it much more reliable and guarantees to Swiss hydro-producers that they can use the flexibility of their plants and seize financial opportunities almost whenever such opportunities occur.

In the last section of this report, we finally focused on the situation in Valais. More than a third of the Swiss hydroelectric capacity is in Valais. The transmission network there is well developed, however, almost all connections right now are at 220kV. The new Nant-de-Drance power plant will be commissioned in the near future and connected to the 380kV network. There will be a 0.9GW increase of the injected power at that voltage level. In the 2015 grid, there is a single 380kV line exiting Valais. If that line fails, the production must be transformed to 220kV at the Chamoson substation which very often (almost always) leads to the overload of the Chamoson transformer. The new lines in the strategic grid 2025 fix that problem and even give a comfortable margin in worst case $N - 1$ computations. We conclude that with its strategic grid 2025, Swissgrid will guarantees reliability of the grid and ensure indiscriminate energy exchanges, even under the exceptional situations considered above.

We note finally that this report says nothing about whether the strategic grid 2025 is optimal from the point of view of investments – we have not investigated if similar results could have been obtained with fewer upgrades. Nevertheless it seems to us that investments planned in Valais are adequate. A CHAMO1-CHIPP1 connection with a smaller capacity by about 20 % or more would still guarantee a high level of grid reliability. We note that such a connection was originally planned by Swissgrid, but that it had to be upgraded to the current capacity of 3.8 GW to reduce noise emissions, following a federal court decision.

- [1] M. Emery, “Le réseau stratégique 2025 de swissgrid,” *Bulletin SEV/VSE*, 2016.
- [2] L. Pagnier and P. Jacquod, “A predictive pan-european economic and production dispatch model for the energy transition in the electricity sector,” in *PowerTech, 2017 IEEE Manchester*, IEEE, 2017.
- [3] P. Jacquod and L. Pagnier, “Le paradoxe de la transition énergétique,” *Bulletin Électrosuisse*, 2017.
- [4] J. B. Ward, “Equivalent circuits for power-flow studies,” *Electrical Engineering*, vol. 68, pp. 794–794, Aug. 1949.
- [5] W. F. Tinney and J. M. Bright, “Adaptive reductions for power flow equivalents,” *IEEE transactions on power systems*, vol. 2, no. 2, pp. 351–359, 1987.

- [6] A. Papaemmanoil and G. Andersson, "On the reduction of large power system models for power market simulations," in *17th Power Systems Computation Conference (PSCC)*, pp. 1308–1313, 2011.
- [7] D. Shi and D. J. Tylavsky, "A novel bus-aggregation-based structure-preserving power system equivalent," *IEEE Transactions on Power Systems*, vol. 30, no. 4, pp. 1977–1986, 2015.
- [8] A. Gómez-Expósito, A. J. Conejo, and C. Cañizares, *Electric energy systems: analysis and operation*. CRC Press, 2008.
- [9] G. Czisch, *Szenarien zur zukünftigen Stromversorgung: kostenoptimierte Variationen zur Versorgung Europas und seiner Nachbarn mit Strom aus erneuerbaren Energien*. PhD thesis, 2005.
- [10] K. Schaber, F. Steinke, and T. Hamacher, "Transmission grid extensions for the integration of variable renewable energies in europe: Who benefits where?," *Energy Policy*, vol. 43, pp. 123–135, 2012.
- [11] F. Comaty, A. Ulbig, and G. Andersson, "Ist das geplante Stromsystem der Schweiz für die Umsetzung der Energiestrategie 2050 aus technischer Sicht geeignet?," 2014.
- [12] R. A. Rodriguez, S. Becker, and M. Greiner, "Cost-optimal design of a simplified, highly renewable pan-european electricity system," *Energy*, vol. 83, pp. 658–668, 2015.
- [13] J. Schippe, A. Seack, and C. Rehtanz, "Pan-european market and network simulation model," in *PowerTech (POWERTECH), 2013 IEEE Grenoble*, pp. 1–6, IEEE, 2013.
- [14] L. Pagnier and P. Jacquod, "How fast can one overcome the paradox of the energy transition? a predictive physico-economic model for the european power grid," *arXiv:1706.00330*, 2017.
- [15] B. von Kupsch, "Bericht zum strategischen Netz 2025," tech. rep., Swissgrid, 2015.
- [16] ENTSO-E, "Entso-e transparency platform." <https://transparency.entsoe.eu>.
- [17] ENTSO-E, "Mid term adequacy forecast." <https://www.entsoe.eu/outlooks/maf/Pages/default.aspx>.
- [18] ENTSO-E, "Tyndp 2016 scenario development report." <http://tyndp.entsoe.eu/>.
- [19] MeteoSwiss, "IDAweb database." <https://gate.meteoswiss.ch/idaweb/>, 2017.